NBS
PUBLICATIONS

NAT'L INST. OF STAND & TECH
A11107 390820

NBSIR 84-2906

Thickness Effect in Low-Density Insulation

Department of Mechanical Engineering
Colorado State University
Fort Collins, CO 80523

August 1984

Prepared for

Department of Energy
Office of Building Energy Research and Development
Building Energy Research and Development
Building Systems Division
Washington, DC 20585

and

U.S. DEPARTMENT OF COMMERCE
National Bureau of Standards
National Engineering Laboratory
ter for Building Technology
thersburg, MD 20899

QC
100
.U56
84-2906
1984
c. 2

NATIONAL BUREAU
OF STANDARDS
LIBRARY

Circ
QC100
.U56
no. 84-2906
1984
c.2

NBSIR 84-2906

THICKNESS EFFECT IN LOW-DENSITY INSULATION

P. J. Burns

Department of Mechanical Engineering
Colorado State University
Fort Collins, CO 80523

August 1984

Prepared for
Department of Energy
Office of Building Research and Development
Building Energy Research and Development
Building Systems Division
Washington, DC 20585

and

U.S. DEPARTMENT OF COMMERCE
National Bureau of Standards
National Engineering Laboratory
Center for Building Technology
Gaithersburg, MD 20899

U.S. DEPARTMENT OF COMMERCE, Malcolm Baldrige, ***Secretary***
NATIONAL BUREAU OF STANDARDS, Ernest Ambler, ***Director***

PREFACE

This report is one of a series documenting NBS research and analysis efforts to support the Department of Energy/National Bureau of Standards' Measurements Program. The work reported in this document was performed cooperatively and supported by DoE/NBS Task Order A008 under Interagency Agreement No. DE-AI01-76PR06010.

ABSTRACT

A discussion is presented of theory of heat transfer in low-density, glass-fiber insulation via conduction, convection, and radiation. It is concluded that the primary modes of heat transfer in this material are air conduction and radiation. An analysis of NBS data of measured apparent thermal conductivity for different thicknesses results in a parameter estimate of the optical extinction coefficient. This parameter determines the amount of change in apparent thermal conductivity as a function of sample thickness. This phenomena is referred to as the "thickness effect."

Keywords: conduction; convection; guarded-hot-plate; low-density insulation; thermal conductivity; thermal radiation; thickness effect.

ACKNOWLEDGMENT

The present work was supported by the Department of Energy and National Bureau of Standards. The National Bureau of Standards also provided high quality data necessary as input to the present approach. Many thanks are also due to Brian Rennex for his valuable comments and practical expertise. Finally, the author wishes to thank Frank Powell, who made the entire project possible.

Nomenclature

A = area (m^2);

e = blackbody emissive power, $\sigma T^4 (W \cdot m^{-2})$;

f_v = volume fraction, defined by equation (3);

g = gravitational constant, 9.8 ($m \cdot s^{-2}$);

I_t = non-dimensional temperature integral defined in equation (25);

K = permeability (m^2);

k = thermal conductivity ($W \cdot m^{-1} \cdot K^{-1}$);

L = thickness of insulation (m);

n = iteration counter;

Nu = Nusselt number;

P = porosity;

$\dot{Q}$ = heat flow (W);

$\dot{q}$ = heat flux ($W \cdot m^{-2}$);

R_k = ratio of conductivities, k_a/k_g;

R_a* = modified Rayleigh number, defined by equation (5);

R^2 = goodness of fit parameter, defined by equation (9);

T = temperature (K);

ΔT = temperature difference, $T_1 - T_2$(K);

x = non-dimensional spatial coordinate, X'/L;

x' = dimensional spatial coordinate (m);

x_1 = first unknown parameter ($kg \cdot m^{-2}$);

x_1' = linearized (old) value of the first parameter ($kg \cdot m^{-2}$);

y_k = measured value;

Greek Symbols

α_o = stagnant thermal diffusivity ($m^2 \cdot s^{-1}$);

β = mass attenuation coefficient ($m^2 \cdot kg^{-1}$) or coefficient of cubical expansion (K^{-1});

γ = second unknown parameter ($W \cdot m^{-1} \cdot K^{-1}$);

δ = deviation;

ε = emissivity;

ν = kinematic viscosity ($m^2 \cdot s^{-1}$);

ρ = density ($kg \cdot m^{-3}$);

σ = standard deviation;

τ_o = optical depth, defined by equation (12).

Subscripts

a denotes air or "in the air"

c denotes convection or critical

e denotes effective

g denotes glass

i denotes insulation

j denotes j'th value

k denotes conduction or k'th iteration

l.s. denotes least squares

m denotes metering section

r denotes radiation

t denotes total (i.e. the entire 48" x 48" sample)

w denotes at the wall

0 denotes stagnant

1 denotes the hot surface

2 denotes the cold surface

Table of Contents

1. THICKNESS EFFECT IN LOW-DENSITY INSULATION

1.1 INTRODUCTION

Determining the heat transfer through porous insulating materials has long been a subject of concern. In particular, judicious engineering design requires the minimization of the total cost associated with the purchase of insulation. This total cost includes the base cost of the insulation and the total cost of the energy that flows through the insulation. The base cost consists of the material cost and the installation cost. Furthermore, the cost of the energy that is transmitted through the insulation must be amortized over the lifetime of the insulation, and it is convenient to perform this minimization in terms of net present worth.

Indeed, to effect the minimization, it is necessary to characterize the performance of the insulation with parameters that can be associated with cost. Thus, the thermal performance of insulating materials is presently characterized versus the density of the sample and the mean diameter of the fibers comprising the porous matrix [1]. Moreover, such has been the practice for some time, as many have analytically addressed [2-5] the problem of modeling the thermal performance of insulating materials, and the experimental investigations are legion [4-8] also. Recently, the research emphasis has been dedicated towards determining the "thickness effect" [8-11], that is, the change in the effective thermal conductivity with specimen thickness. In particular, a very detailed discussion of the thickness effect may be found in Reference 11. In connection with this, it is noteworthy that the effective thermal conductivity can be well-characterized [12] versus percent light transmission.

To date, the problem has been addressed only deterministically in that physical mechanisms have been assumed, ranges of transfer coefficients have been selected, and solutions have been obtained under a wide variety of simplifying assumptions. This technique yields excellent insight when determining the relative effects of various physical mechanisms, but it is sometimes fruitless to attempt to accurately predict the actual heat transfer occurring in a specific physical system because the predicted property (in this case the effective thermal conductivity) may vary much more under the range of input parameters than does the observed experimental data. Actually, this can be attributed both to the variation due to the approximate nature of the solutions, and due to the lack of knowledge of the specific input parameters. In particular, the solid conduction contribution will change depending upon the assumptions made as to fiber orientation, and the radiative parameters (phase function and extinction and single scattering coefficients) are not well known for general situations. The adhesive binder is a complicating factor of great physical importance that is usually neglected in theoretical analyses, and there is likely to be large spatial variations in binder content in any one batch of insulation. There is also likely to be large global variations in binder content from batch to batch. Thus, the law of diminishing returns is operating in that further deterministic analyses will be very tedious and will yield less practical information than those of the past.

In this light, a stochastic approach will be undertaken herein that will circumvent many of these difficulties and yield some new insight into the experimental determination of the effective thermal conductivity. In short, relationships for heat transfer modes will be assumed in terms of unknown constants. These unknown constants will, in effect, be the uncertain parameters mentioned above. Since these parameters will be determined from the data, they will automatically be the "best-fit" values consistent with the assumed model and the scatter in the data. The true test of this method will entail comparison of the overall scatter in the data against the scatter in the predicted values. Also, enough data points must be used to ensure a statistically significant result. Both of these facets of the present approach will be quantified.

Because the parameters will be derived from experimental data obtained at the NBS in Gaithersburg, MD, a few comments concerning the quality and the material variability of the insulation samples are in order. Figure 1, which was abstracted from Reference 13, shows that both density and fiber diameter are important parameters in determining the effective thermal conductivity of fibrous insulations. The data used herein are NBS-measured values taken from the calibrated transfer samples prepared for the NBS by the Johns Manville Corporation. These samples vary widely in thickness and density, yet the fiber diameters were controlled very carefully to have a mean value of 3.8×10^{-6} m for all of the samples. Further detail may be found in Reference 1. Thus, we shall proceed realizing that the fiber diameter is a parameter which is held fixed in the present analysis. The most that can be done, then, is to predict the thickness effect at a constant fiber diameter. For completeness, Table 1 includes values of the datum points used.

The present analysis will proceed in the following vein. Physical mechanisms for the heat transfer will be examined and proposed, and detailed discussions of past models are given. A brief description of the sequential least squares algorithm follows. The data are then filtered through a variety of models, and the present work ends with conclusions and recommendations.

2. HEAT TRANSFER OVERVIEW

2.1 THEORETICAL FORMULATION

The problem under consideration is to predict the heat flow through low density insulation given the boundary conditions (the boundary temperatures). Of course, the basic material properties must also be known as they are required input parameters. The heat flow will be assumed to be one-dimensional as the NBS GHP (Guarded Hot Plate) satisfies very stringent criteria in this regard (about 0.1 percent accuracy). In this case, the heat flow may be conceptualized as follows:

$$\dot{Q} = \dot{Q}_k + \dot{Q}_c + \dot{Q}_r + \dot{Q}_{kc} + \dot{Q}_{kr} + \dot{Q}_{rc} \quad (1)$$

where separate contributions have been included for conduction (k), convection (c), and radiation (r). Also, interactions between all three modes of heat transfer have been allowed as separate terms and it is presumed that these terms are of smaller magnitude than the ones involving the basic modes of heat transfer. The validity of this assumption will be demonstrated by the match between thing and experiment. The terms will be addressed one-by-one.

2.2 CONDUCTION

The conduction term, $\dot{Q}_k$, involves the gaseous and solid conduction through the porous medium. There is also an interaction term associated with these two modes of conduction. This can be conceptualized as follows: since the contact areas between fibers are small, the constriction resistance is large and little heat flows through the solid matrix directly. However, if the fibers do contact or if they come close together, heat will flow from one fiber through the intervening gas to another fiber. A careful analysis of this process for packed spheres [14] shows that this, in fact, is a major transfer mechanism for heat flowing through the solid. Indeed, a number of analytical investigators [2-5, 9, 10, 14-16] have pursued this subject. Experimental treatments of this topic [2-8] confirm most of the theories for low density porous insulation wherein the solid matrix is so widely dispersed (porosity = 0.995) that only a small portion of heat flow can be attributed to the fibers. This is readily evident by viewing Figure 2, which has been abstracted from the review article by Bankvall [5]. The model used herein is one proposed by Bhattacharyya [10]:

$$\dot{Q}_k = k_g A \frac{\Delta T}{L} \alpha_k \; \frac{1 - \dfrac{1 - R_k}{1 + 2 R_k f_v}}{1 + R_k} + (1-\alpha_k)\left[1 - \frac{\dfrac{1 - R_k}{1 + f_v(1 + 5R_k)}}{3(1 + R_k)}\right] \quad (2)$$

where, for air at 287K and glass fibers, the properties are taken as follows: $k_g = 1.04\ \mathrm{W{\cdot}m^{-1}{\cdot}K^{-1}}$, $k_a = 0.026\ \mathrm{W{\cdot}m^{1} \cdot K^{-1}}$, and $\rho_g = 2580\ \mathrm{kg{\cdot}m^{-3}}$, $\rho_a = 1.04\ \mathrm{kg{\cdot}m^{-3}}$. The volume fraction is computed as follows:

$$f_v = \frac{(\rho_i - \rho_a)}{(\rho_g - \rho_a)} \quad (3)$$

2.3 CONVECTION

The convective heat transfer in horizontal porous media has been the subject of extensive investigation for several decades [17-30]. The critical modified Rayleigh number, Ra_c^*, below which no convection can occur in a horizontal porous medium heated from below has been determined to be as follows [17, 18]:

$$Ra_c^* = 4\Pi^2 \cong 39.5 \quad (4)$$

where the modified Rayleigh number qualitatively represents the ratio of the buoyancy force to the drag force of the porous matrix, and is given as:

$$Ra^* = \frac{g\ \beta\ \Delta T\ K\ L}{\nu \alpha_o} \quad (5)$$

wherein the effective thermal conductivity of the stagnant porous medium is used to calculate the thermal diffusivity, α_o. A number of experimental investigations [20, 22-24] have verified the relationship given by equation (4). Elder [24], gives the following formula for the non-dimensional steady convective heat transfer in porous media heated from below:

$$Nu = \frac{\dot{Q}_c + \dot{Q}_k}{\dot{Q}_k} = 1 + (Ra^* - Ra_c^*)/40 \quad (6)$$

where Nu = 1 if $Ra^* \leq Ra_c^*$.

It is of interest to estimate the magnitude of the free convective heat transfer in porous media using equations (4) and (5). First the modified Rayleigh number is calculated. The following values of the parameters are used:

$g = 9.8\ m \cdot s^{-2}$, $\beta = T_m^{-1} = 3.37 \times 10^{-3}\ K^{-1}$, $\nu = 1.56 \times 10^{-5}\ m^2 \cdot s^{-1}$ $k_o^* = 0.045\ W \cdot m^{-1} \cdot K^{-1}$, $\rho = 1.16\ kg \cdot m^{-3}$, $c_p = 1.011\ J \cdot kg^{-1} \cdot K^{-1}$, $\alpha_o = 3.84 \times 10^{-5}\ m^2 \cdot s^{-1}$, $L = 0.1562\ m$, $K = 5 \times 10^{-8}\ m^2$.**

These values result in a modified Rayleigh number of:

$$Ra^* (\Delta T) = 0.419\ \Delta T (K)^{-1} \quad (7)$$

For the ΔT = 27.8K used in the GHP, the modified Rayleigh number is:

$$Ra^* (27.8) = 11.6 \quad (8)$$

which is below the critical value, so all of the terms associated with convection in equation (1) are nil. Indeed, setting equation (7) equal to

---

* Taken from measurements made using the NBS Guarded Hot Plated [1].

** Taken from Fournier and Klarsfeld [7], Fig. 5, F = 3.6 (typical of the 3.8 μm diameter fibers in the measurement system of [1]).

equation (4) results in a $\Delta T = 95.9K$ for the onset of convective flow. Thus, free convection is seen to be a significant contributor to the heat transfer for porous insulations only at very large thicknesses and very large temperature differences. Indeed, for all practical cases of thermal insulation at room temperature, free convection heat transfer does not occur in the horizontal geometry.

2.4 RADIATION

As seen by viewing Figure 2, radiation heat transfer contributes significantly to the total heat transfer in low density fibrous insulation. Recent theoretical calculations neglecting the phenolic binder [31] show that the scattering coefficient is roughly a factor of 2 to 4 times larger than the absorption coefficient, but this conclusion has not been conclusively supported with experimental data. Indeed, there is some indication that the phenolic binder is highly absorptive. Moreover, it is extremely difficult to measure absorption and scattering coefficients separately [32-33], especially in the midst of a matrix of solid fibers. Despite these limitations, a brief review of past work in this area will be presented for illustrative purposes.

The pioneering work was done by Hamaker [34] and Larkin and Churchill [35] who applied the two flux model for gray absorbing and scattering media. The approximation of radiative equilibrium used does not allow free interaction between the radiation and conduction which limits the general applicability of their results. Viskanta subsequently pursued the problem including isotropic scattering from a more rigorous standpoint for the condition of radiative equilibrium [36], and later coupled with conduction [37]. It is mentioned in passing that

Usiskin and Sparrow [38], and Heaslet and Warming [39] presented a solution for a purely absorbing medium. Furthermore, the diffusion technique has also been applied to the problem [46] of radiation heat transfer in a purely absorbing medium.

Some further analyses into the problem at hand have attempted to remove the assumption of isotropic scattering [41-43], enhance the applicability of the two-flux assumption [44, 45] or include transients [46]. Further analytical work may be found in Reference 47, wherein a large parameter variation was performed. All of the investigations mentioned so far assume gray material properties.

Recently, Tong and Tien [31] have applied a two-flux model to the specific problem involving glass fibers wherein the spectral solution of Maxwell's equations have been used to determine the absorption and scattering coefficients. While this represents a large step in the right direction, the questions of fiber orientation and the effect of the adhesive binder are still to be included in a more rigorous analysis. Furthermore, it is questionable whether such an approach involving an approximate solution technique can ever be predictive to within, say, two percent as is necessary to predict the thickness effect.

It is therefore concluded that the research community has yet to accurately solve the generalized equation of transfer for the specific problem of radiant heat transfer in fibrous insulations with binder present. Furthermore, the property measurements that have been made [e.g., extinction coefficient] must be augmented by further measurements including the single scattering albedo [32-33] to be generally applicable to the present problem. Indeed, this is not an easy problem either as the question of the separation of effects when measuring quantities that can be attributed to diverse physical mechanisms is an elusive one [48].

Rather, the approach adopted here will consist of taking the measured data for heat transfer rates, assuming physical models and filtering the measured data through the assumed model to attain "best-fit" values for the thermal parameters. This approach has the advantages of yielding the best thermal parameters that pertain to the data at hand consistent with the noise level of the data, the assumed model and, of course, the minimization of the L-2 norm. However, the approach cannot truly be called deterministic as the material properties are derived from performance data rather than vice versa, but this is a philosophical and not a technical issue and, consequently, will not be further addressed. Instead, the pitfalls inherent in such an attempt will be discussed, and it will become evident that the range of applicability of the generated parameters will be pronouncedly affected by the specific models assumed and by the specific data filtered.

3. ANALYSIS

3.1 PARAMETER ESTIMATION

When parameter estimation is employed to determine thermal parameters, two general rules must be separately observed in order to obtain meaningful results. Firstly, the model must be representative of the physical processes occurring in the experimental system. For example, problems are sometimes encountered when free convection ($T^{1/3}$ dependence) and radiation (T^3 dependence) are erroneously lumped into the same heat transfer coefficients in a model. This type of model will not allow modes to be identified. Also, all terms of significance must be included in the model. If convection is indeed an important mode of heat transfer, its effects will be contained in the data, and when the data are analyzed, these effects will be attributed to some parameters, and incorrectly so if convection is not represented in the model.

Secondly, the combination of the noise level of the data and the number of data samples taken must be such as to render the results statistically homogeneous. The general rule of thumb is that the noise level of the data should be much less than the signal level of the physical mechanism that is to be identified. This stringent criterion may be relaxed as larger numbers of datum points become available. Other problems that are specific to each individual problem under investigation [47] will not be addressed here.

3.2 SEQUENTIAL FORMULATION

The formulation of the sequential linear least squares algorithm is well-developed elsewhere [48] and will not be repeated here. Instead, the use of the technique will be presented by example. Suppose that j parameters x_j are to be identified from the measured values A, which multiply the parameters and y, which appear separately. Mathematically,

$$A_{kj} x_j = y_k \qquad (9)$$

where k denotes the k'th measurement. The system becomes overdetermined when k becomes greater than j, and no general solution is then possible. Rather, the system must be solved for the parameters that satisfy some global criterion. It is convenient to choose this criterion to be the minimization of the L-2 norm of the errors in the parameters.

When identifying j parameters, the linear system of equations becomes complete when j experimental observations have been added to the system. The equations can be solved at this time by Gaussian elimination, yielding a set of parameters that are representative of the measurements taken. When these measurements contain significant noise, the parameters are likely to be substantially in error at this point. In order to yield physically realistic parameters, additional data points are processed.

However, as one more observation is added to the set, the system becomes overdetermined. Then, least squares procedures are used. Least squares data processing will yield a new set of parameters each time an additional observation is processed. This is possible to do with ordinary least squares algorithms by reformulating and reducing the A matrix each time. The sequential least squares algorithm performs this function at a fraction of the computer time because the matrix does not get reformulated and reduced for each data point. Thus, sequential least squares yields values for the parameters after each data observation is added.

This is advantageous in two ways. First, by observing the parameter trajectories, it can usually be determined whether enough data points have been processed for the noise to be filtered out. Secondly, it can sometimes be determined whether there are imperfections in the model. To explain this, consider the situation where data have been taken on a 0.05 m specimen. Suppose that the initial noise in the parameters has died out, and the parameter trajectories have been observed to become flat. Suppose, further, that data from a 0.1 m sample are next added. If the parameter trajectories are observed to suddenly start to change and continue to change steadily, it can be deduced that there is error in the model as it does not fit all the different physical situations in a similar fashion. This is termed "model noise." Thus, the model should be reformulated and the data reprocessed until a uniformily valid set of parameters is obtained.

In summary, a sequential observation of the parameter trajectories can be useful in detecting model noise and in determining when a sufficient number of data observations have been processed to overcome the experimental noise level. The sequential algorithm is given for reference in the Appendix.

3.3 APPLICATIONS

The problem at hand is formulated in terms of the effective thermal conductivity as follows:

$$k_e = k_k + k_r \tag{10}$$

where k_k is the term in brackets in equation (2). It is for pure conduction thru the solid and air.

The radiation conductivity is taken to be as follows:

$$k_r = \frac{\sigma(T_1^2 + T_2^2)(T_1 + T_2)L}{\frac{1}{\varepsilon_1} + \frac{1}{\varepsilon_2} - 1 + 3\,\tau_o/4} \tag{11}$$

where all of the quantities in equation (11) are assumed to be measured except for τ_o, the effective optical depth. This parameter is termed effective in that it incorporates the effects of absorption, anisotropic scattering, spectral properties, fiber orientation and the binder material. It is standard practice to determine the properties of fibrous insulation (i.e. the effective thermal conductivity and the permeability) as a function of the material density, ρ. Since the scattering of radiation is proportional to the number of scattering particles within the medium, it is reasonable to assume that:

$$\tau_o = \beta \rho L \tag{12}$$

Further, it is known [1] that:

$$\frac{1}{\varepsilon_1} + \frac{1}{\varepsilon_2} - 1 << \frac{3}{4}\tau_o \tag{13}$$

Equations (11) and (12) may be combined together with the condition stipulated as equation (13) and the binomial theorem to yield:

$$k_r = x_1 \frac{4\sigma(T_1^2 + T_2^2)(T_1 + T_2)}{3\rho} \left[1 - x_1' \frac{4(1/\varepsilon_1 + 1/\varepsilon_2 - 1)}{3\rho L}\right] \tag{14}$$

where the term has been linearized by the inclusion of the old value of the parameter x_1'. Also:

$$x_1 = \beta^{-1} \tag{15}$$

It is apparent that it is necessary to iterate to determine a "thickness effect" as it only shows up in equation (14) as a product involving the old value, x_1', of the radiation parameter. Thus, x_1' is set to zero (the first old value), x_1, is determined; the old value x_1' is next set to this value of x_1; the filtering is performed again yielding a new value of x_1 and the procedure continues until convergence is achieved. Finally, it is noted that equation (11) is similar in form to the derivations of Verschoor and Greebler [2], Bankvall [5], van der Held [50], Hager and Steere [51], and Strong et. al. [52].

The geometry for the first problem is shown in Figure 3. At the low densities at which the present data exist, solid conduction plays very little role in the heat transfer, and, therefore, the conductive contribution was modeled as in equation (2), and taken as a known quantity (i.e., included in the right-hand side).

The linearized multiplier for the radiative parameter is explicitly:

$$A_{k1} = \frac{4\sigma(T_1^2 + T_2^2)(T_1 + T_2)}{3\rho}\left[1 - x_1' \frac{4(1/\varepsilon_1 + 1/\varepsilon_2 - 1)}{3\rho L}\right] \tag{16}$$

Finally, the known quantity including the effective thermal conductivity, k_e, is explicitly:

$$y_k = k_e - \dot{Q}_k L/(\Delta T\ A) \tag{17}$$

where the second term (= k_k) is calculated using equation (2).

Figure 4 shows the variation of x_1, with the number of datum points, n. Recall that a sequential filter generates the "best-fit" value for the parameter being estimated for each sequence of datum points up to and including the present one. The data are organized from left to right as the 0.0254 m (1") set, the 0.0381 m (1.5") set, the 0.0762 m (3") set and the 0.1524 m (6") set. Local variations are seen to be extreme below n = 10 and are observed to damp out for n>20 due to the averaging of a larger number of points. Thus, it may be concluded that there are more than enough data points to render local fluctuations (measurement noise) insignificant. However, the global variation (model noise) of the parameter manifested as a decrease in x_1 with an increase in thickness (negative slope) is disturbing. This suggests that the proposed model for the effective thermal conductivity is of the wrong form else the parameter, x_1, would have leveled off. Obviously, relative to the value of x_1, at a thickness of 0.0254 m (1"), the value of x_1, for a thickness of 0.1524 m (6") should be lower. Thus, although the family of predicted curves should nestle close to the average of the experimental data, the thickness effect will not be well represented.

This is indeed observed in Figure 5 which presents the predicted curves and the experimental data points for the four thicknesses of interest. While the average values have been predicted well, the thickness effect has been overpredicted. The 0.0254 m (1") curve lies on or below all of the 0.0254 m (1") data but one point. The 0.0381 m (1.5") curve is statistically unimportant as there are only 3 data points appertaining thereto. The 0.0762 m (3") curve appears to be a good fit for its data and the 0.1524 m (6") curve lies above all of its associated data points but one. For the data shown, the thickness effect is eyeballed to be about 3.5 percent at $\rho = 9 kg \cdot m^{-3}$) while the predicted curves indicate a thickness effect of about 6 percent.

Several comments are appropriate here. First of all, the value of $\beta = 39.5$ $m^2 \cdot kg^{-1}$ is the best value of β consistent with the present model for the given experimental data. Secondly, even though the scatter in the data is substantial, it is apparent from Figure 6 that the thickness effect is overpredicted. Finally, the additional correction required to bring the predictions in line with the data is small (about 2.5 percent), and, therefore, may be attributed to a variety of factors. The approach taken is to attribute the discrepancy to the most obvious physical mechanism. The merit of this assumption can then be judged by the final results obtained.

Insight may be gained by viewing the predicted temperature profiles. Since radiative and conductive heat transfer have been treated separately, the temperature profiles are plotted separately with the caveat that since about half the heat transfer is due to radiation and half is due to conduction, the initial predicted temperature profile may be roughly taken as the average of the two. The conduction temperature profile, T_k, is taken as linear from

T_2 = 283.0 K to T_1 = 310.3 K as shown in Figure 6. The radiation temperature profile was derived by Deissler [40], and will be presented here in brief. The jump in emissivity at surface 2 is given as:

$$e_{a2} = e_{w2} + (e_{w1} - e_{w2})(1/\varepsilon_2 - 0.5) \tag{18}$$

The blackbody emissivity power then varies linearly (with x) through the medium, viz:

$$e_a(x) = e_{a2} + x \frac{0.75\rho\beta L \ (e_{w1}-e_{w2})}{0.75\rho\beta L + 1/\varepsilon_1 + 1/\varepsilon_2 - 1} \tag{19}$$

Combining the two previous equations, the temperature profile in the medium is determined as:

$$T_r = \{\frac{e_{w2}}{\sigma} + \frac{(e_{w1} - e_{w2})}{\sigma}[\frac{1}{\varepsilon_2} - 0.5 + \frac{0.75\rho\beta L \ x}{0.75\rho\beta L + 1/\varepsilon_1 + 1/\varepsilon_2 - 1}]\}^{1/4} \tag{20}$$

The profiles of T_r are shown in Figure 6 for the four thicknesses of interest where the parameters have been taken as $\rho_i = 9$ kg·m^{-3} and $\varepsilon_1 = \varepsilon_2 = 0.9$. The jump boundary conditions result in an increase above T_k at x = 0 and a decrement below T_k at x =1. There is clearly a significant increase in the average temperature when radiation is considered, and it is observed that the radiation profiles are nonlinear. Conduction will have the following two effects on the radiative temperature profile: (1) it will eliminate the jump at the boundaries, and (2) it will tend to smooth the overall profile by transferring heat through the insulation. This second effect will serve to reduce the magnitude of the temperature difference from conduction and, hence, will reduce the thickness effect. This is precisely the type of mechanism needed to enhance the present theory.

Attention is therefore focused upon the coupling between the radiative and the conductive profiles. Since the effects are small, the base solutions as given above will be used, similar to perturbation theory, to determine the coupled heat transfer. The initial approach taken was to integrate the radiative temperatures excess (as a function of position) divided by the conduction length to the cold wall. This approach did not bear fruit as the temperature jump at the cold wall rendered the integrand and subsequently the integral infinite. Since the conduction will eliminate the jump, the mathematics is not inconsistent with the physics of the situation. Next, it was reasoned that the contribution to the effective thermal conductivity of the coupling between radiation and conduction should be proportional to the absolute magnitude of the average radiative temperature excess, i.e.:

$$k_{cr} = \gamma \int_{x=0}^{x=1} \frac{T_r - T_c}{T_1 - T_2} dx \qquad (25)$$

This integral, denoted as the non-dimensional temperature integral, I_T, is shown in Figure 7, as a function of density for the four thicknesses of interest with $\varepsilon_1 = \varepsilon_2 = 0.9$ and $\beta = 4\ m^2 \cdot kg^{-1}$. The graph appears to be consistent with the observed data, i.e., the curves decrease with increasing density and the effects are more pronounced at lower thicknesses.

The approach taken is to apply the sequential least squares filtering technique to estimate γ in equation (21). Since this term is likely to be small, the filtering is done for this term alone to avoid possible computational "conditioning" problems. Thus, the conduction and the primary radiation terms are taken to the right-hand-side of the equations as knowns, with an assumed β. The sequential filtering is then done for a variety of values of β, resulting in a variance, σ^2, for each assumed β. This corresponds to hunting around in the two space of (γ,β) for the overall minimum, and is illustrated graphically in Figure 8. The minimum is achieved for $\beta = 44.0\ m^2 \cdot kg^{-1}$, and the corresponding "best-fit" value of γ if $\gamma = 0.0740\ W \cdot m^{-1} \cdot K^{-1}$. Recall that a correction of about $0.0015\ W \cdot m^{-1} \cdot K^{-1}$ is being sought, and the integral, I_T, was shown to have a value of about 0.025. Thus, γ appears to be of the correct magnitude.

The new relationship is presented together with the experimental data in Figure 9 for the four thicknesses. The predicted thickness effect is now seen to be consistent with the experimental data. Moreover, it appears that the thickness effect is delineated about as much as possible given the scatter of the data. Two datum points from the curve fit of Rennex [11] at the two thicknesses of 0.0254 m (1") and 0.1524 m (6") are shown for $\beta = 44\ m^2 \cdot kg^{-1}$ as open and closed hexagons, respectively. The thickness effect is about the same as is predicted by the present analysis, but these values lie well below the present data. The lower values are attributed to the fact that the value of β used in the calculation is different from the one that would be obtained by filtering using his curve fit. This illustrates that the "best-fit" parameters for one model are not necessarily the "best-fit" values for another model. Using the previous value of $\beta = 39.5\ m^2 \cdot kg^{-1}$, the open hexagons are plotted for all densities and at the thicknesses of 0.0254 m (1") and 0.1524 m (6") with a double-dashed line and a triple-dashed line, respectively. From this, it is observed that the Rennex-curve fit slightly overpredicts the thickness effect for the present data set, but the overall agreement is good.

4. CONCLUSIONS AND RECOMMENDATIONS

Conduction has been shown to be essentially that of stagnant air, and convection has been demonstrated to be nonexistent in horizontal building insulation under the usual circumstances encountered in practice. Radiation was found to contribute approximately one-half to the total heat transfer. A relation of the diffusion approximation genre was found to be inappropriate in form to predict the thickness effect. The inclusion of a term to account for the conductive-radiative interaction was found to represent the data well. The present approximation was found to be slightly better for the present data set than the curve fit of Rennex [11]. For completeness, the entire relationship is presented as follows:

$$k_c = k_k + k_r + \gamma I_T \tag{22}$$

where the conductive contribution is given as [10]:

$$k_c = k_g \quad \alpha_k \left(1 - \frac{1 - R_K}{1 + \frac{2R_K f_v}{1+R_k}}\right) + (1-\alpha_k) \quad \left(1 - \frac{1 - R_K}{1 + \frac{f_v(1 + 5\ R_K)}{3(1 + R_k)}}\right) \tag{23}$$

and the radiative term is as follows [40]:

$$k_r = \frac{\sigma(T_1{}^2 + T_2{}^2)(T_1 + T_2)L}{3\ \rho\beta L/4 + 1/\varepsilon_1 + 1/\varepsilon_2 - 1} \tag{24}$$

The values of the constants are given as follows:

$$\beta = 44.0\ m^2\cdot kg^{-1} \tag{25}$$

$$\gamma = 0.0740\ W\cdot m^{-1}\cdot K^{-1} \tag{26}$$

$$\alpha_k = 0.5 \tag{27}$$

The present approach predicts the thickness effect very well from a firm fundamental basis. The universal merit of the present result can only be assessed when the technique has been applied to an inclusive data set including different fiber diameters (most especially), different surface temperatures, and a wider variation of densities. Also, the variation in types and quantities of binders is a complicating factor.

5. REFERENCES

1. B. G. Rennex, "Low-Density Thermal Insulation Calibrated Transfer Samples-A Description and a Discussion of the Material Variability," NBSIR-82-2538 (1982).

2. J. D. Verschoor and P. Greebler, "Heat Transfer by Gas Conduction and Radiation in Fibrous Insulations," ASME Trans., 74, p. 961 (1952).

3. R. H. E. Brailey, "Heat Flow Through Insulations Used in the Chemical Process Industry," presented at the Symposium on Glass and Related Materials, II, AICHE Preprint 32E, Phila. PA (1968).

4. C. Bankvall, "Heat Transfer in Fibrous Materials," J. Testing and Evaluation, 1, p. 235 (1973).

5. C. Bankvall, "Mechanisms of Heat Transfer in Permeable Insulation and Their Investigation in a Special Guarded Hot Plate," Heat Transmission Measurements in Thermal Insulations, ASTM STP 544, p. 34 (1974).

6. C. M. Pelanne, "Experiments on the Separation of Heat Transfer Mechanisms in Low-Density Fibrous Insulation," Proc. Eighth Thermal Conductivity Conf. Plenum Press, New York (1969).

7. D. Fournier and S. Klarsfeld, "Some Recent Experimental Data on Glass Fiber Insulating Materials and Their Use for A Reliable Design of Insulations at Low Temperatures," Heat Transmission Measurements in Thermal Insulations, ASTM STP 544, p. 223 (1974).

8. C. M. Pelanne, "Experiments to Separate the 'Effect of Thickness' from Systematic Equipment Errors in Thermal Transmission Measurements," presented at the ASTM C 1600 Thermal Insulation Conference, Tampa, FLA, (Oct. 1978).

9. C. J. Shirtliffe, "Effect of Thickness on the Thermal Properties of Thick Specimens of Low-Density Thermal Insulation," Thermal Insulation Performance, ASTM STP 718, p. 36 (1980).

10. R. K. Bhattacharyya, "Heat Transfer Model for Fibrous Insulations," Thermal Insulation Performance, ASTM STP 718, p. 272 (1980).

11. B. G. Rennex, "Thermal Parameters as a Function of Thickness for Combined Radiation and Conduction in Low-Density Insulation," Journal of Thermal Insulation, 1, p. 283 (1981).

12. C. M. Pelanne, "Thermal and Physical Characteristics of Glass Fiber Insulation Produced for the National Bureau of Standards." Johns Manville Report 436-T-1528 (April 1981).

13. ASHRAE Handbook of Fundamentals (1981), p. 205.

14. Y. Ogniewicz and M. M. Yovanovich, "Effective Conductivity of Regularly Packed Spheres: Basic Cell Model with Constriction," AIAA paper 77-188 (1977).

15. Luikov, et. al., "Thermal Conductivity of Porous Systems," Int. J. Heat Mass Transfer, 11, p. 117-140 (1968).

16. M. E. Stephenson and M. Mark, "Thermal Conductivity of Porous Materials," ASHRAE Journal, pp. 75-81 (1961).

17. A. Pellew and R. V. Southwell, "On Maintained Convective Motion in a Fluid Heated from Below," Proc. Royal Soc., A176, p. 312-343 (1940).

18. C. W. Horton and F. T. Rogers, "Convective Currents in a Porous Medium," J. Appl. Physics, 16, p. 367-370 (1945).

19. E. R. Lapwood, "Convection of a Fluid in a Porous Medium," Proc. Camb. Phil. Soc., 44, p. 508-521 (1948).

20. H. L. Morrison, F. T. Rogers and C. W. Horton, "Convective Currents in Porous Media, II. Observation of Condition at Onset of Convection," J. Appl. Physics, 20, p. 1027-1029 (1949).

21. F. T. Rogers, H. L. Morrison, "Convection Currents in a Porous Media, III. Extended Theory of the Critical Gradient," J. Appl. Physics, 21, p. 1177-1180 (1950).

22. F. T. Rogers, L. E. Schilberg and H. L. Morrison, "Convection Currents in a Porous Media, IV. Remarks on the Theory," J. Appl. Phys., 22, p. 1476-1479 (1951).

23. Y. Katto and T. Masuoka, "Criterion for the Onset of Convective Flow in a Fluid in a Porous Medium," Int. J. Heat Mass Transfer, 10, p. 297-309 (1967).

24. J. W. Elder, "Steady Free Convection in a Porous Medium Heated Flow Below," J. Fluid Mech., 27, p. 29-48 (1967).

25. J. W. Elder, "Transient Convection in a Porous Medium," J. Fluid Mech., 27, 609-623 (1967).

26. E. Palm, J. E. Weber and O. Kvernvold, "On Steady Convection in a Porous Medium," J. Fluid Mech., 54, p. 153-161 (1972).

27. F. H. Busse and D. D. Joseph, "Bounds for Heat Transport in a Porous Layer," J. Fluid Mech., 54, p. 521-543 (1972).

28. J. M. Straus, "Large Amplitude Convection in Porous Media," J. Fluid Mech., 64, p. 51-63 (1974).

29. D. R. Kassoy and A. Zebibe, "Variable Viscosity Effects on the Onset of Convection in Porous Media," Phys. Fluids, 18, p. 1649-1651 (1976).

30. R. J. Ribando and K. Torrance, "Natural Convection in a Porous Medium: Effects of Confinement, Variable Permeability, and Thermal Boundary Conditions," Journal Ht. Transfer, 98, p. 42-48 (1976).

31. T. W. Tong and C. L. Tien, "Radiation Heat Transfer in Fibrous Insulation - Part I, Analytical Study," ASME Paper No. 81 - HT-42 (also see T.W. Tong, O. S. Yong and C. L. Tien," Radiative Heat Transfer in Fibrous Insulation - Part II, Experimental Study," ASME Paper 81-HT-43.

32. J. Reichman, "Determination of Absorption and Scattering Coefficients for Nonhomogeneous Media. 1:Therory," Applied Optics, 12, p. 1811-1815 (1973).

33. W. G. Egan, T. Hilgeman and J. Reichman, "Determination of Absorption and Scattering Coefficients for Nonhomogeneous Media. 2:Experiment," Applied Optics, 12, p. 1816-1823 (1973).

34. H. C. Hamaker, "Radiation and Heat Conduction in Light Scattering Materials," Phillips Research Reports, 3, p. 55-67 (1947).

35. B. K. Larkin and S. W. Churchill, "Heat Transfer by Radiation Through Porous Insulations," AICHE Journal, 5, p. 467-474 (1959).

36. R. Viskanta and R. J. Grosh, "Heat Transfer in a Thermal Radiation Absorbing and Scattering Medium," International Dev. in HA Transfer, IV ASME, New York, p. 820-828 (1961).

37. R. Viskanta, "Heat Transfer by Conduction and Radiation in Absorbing and Scattering Materials, Journal Ht. Transfer, 87, p. 143-150 (1965).

38. C. M. Usisken and E. M. Sparrow, "Thermal Radiation Between Parallel Plates Separated by an Absorbing-Emitting Nonisothermal Gas," Int. J. Heat Mass Transfer, 1, p. 28-36 (1960).

39. M. A. Heaslet and R. F. Warming, "Radiative Transport and Wall Temperature Slip in an Absorbing Planar Medium," Int. J. Heat Mass Transfer, 8, p. 979-994 (1965).

40. R. G. Deissler, "Diffusion Approximation for Thermal Radiation in Gasses with Jump Boundary Condition," Journal Ht. Transfer, 86, p. 240-246 (1964).

41. L. B. Evans, C. M. Chu and S. W. Churchill, "The Effect of Anisotropic Scattering on Radiant Transport," Journal Ht. Transfer, 87, p. 381-387 (1965).

42. H. M. Hsiu and T. J. Love, "Radiative Heat Transfer Between Parallel Plates Separated by a Nonisothermal Medium with Anisotropic Scattering," Journal Ht. Transfer, 89, p. 197-204 (1967).

43. A. Dayan and C. L. Tien, "Heat Transfer in a Gray Planar Medium with Linear Anisotropic Scattering," Journal Ht. Transfer, 97, p. 391-396 (1975).

44. S. C. Traugott and K. C. Wang, "On Differential Methods for Radiant Heat Transfer," Int. J. Heat Mass Transfer, 7, p. 269-270 (1964).

45. J. B. Berquam and R. A. Seban, "Heat Transfer by Conduction and Radiation in Absorbing and Scattering Materials," Journal Ht. Transfer, 93, p. 236-239 (1971).

46. C. C. Lii and M. N. Ozisik, "Transient Radiation and Conduction in an Absorbing, Emitting, Scattering Slab with Reflecting Boundaries," Int. J. Heat Mass Transfer, 15, p. 1175-1179 (1972).

47. H. A. Fine, S. H. Jury, D. W. Yarbrough and D. L. McElroy, "Analysis of Heat Transfer in Building Thermal Insulation," Oak Ridge Report ORNL/TM-7481 (1980).

48. D. V. Pryor, "Parameter Estimation for Heat Transfer During Hyperthermia Treatment," Ph-D. Thesis, Colorado State University (in preparation).

49. G. J. Bierman, Factorization Methods for Discrete Sequential Systems, Academic Press, New York, pp. 8-20 (1973).

50. E. F. M. van der Held, "The Contribution of Radiation to the Conduction of Heat, III. Boundary Conditions," Appl. Sci. Res., A4, pp. 77-99 (1953).

51. N. E. Hager, Jr. and R. C. Steere, "Radiant Heat Transfer in Fibrous Thermal Insulation," J. Appl. Phys., 38, pp. 4463-4668 (1967).

52. H. M. Strong, F. P. Bundy and H. P. Bovenkerk, "Flat Panel Vacuum Thermal Insulation," J. Appl. Phys., 31, pp. 39-50 (1960).

Table 1. Experimental Data

Thickness (mm)	k_{eff} ($W \cdot m^{-1} \cdot K^{-1}$)	ρ_m ($kg \cdot m^{-3}$)	ρ_T ($kg \cdot m^{-3}$)
25.27	0.04470	10.03*	10.03
25.46	0.04542	9.47	9.52
25.35	0.04618	9.14	8.92
25.35	0.04617	9.11	9.04
25.35	0.04557	8.83	8.78
25.35	0.04619	9.25	9.98
25.35	0.04810	8.09	8.67
25.35	0.04362	10.67	10.39
25.35	0.04443	9.92	9.91
25.35	0.04427	9.17	10.17
25.38	0.04487	10.56*	10.56
25.35	0.04512	9.13	9.09
25.37	0.04577	9.11	9.39
25.35	0.04568	9.01	9.22
25.38	0.04527	9.63	9.78
25.38	0.04457	10.22	10.79
25.77	0.04377	11.13	11.14
25.77	0.04364	10.88	11.07
38.08	0.04715	9.51	8.64
38.08	0.05030	7.14	7.34
38.15	0.04272	11.40	11.24
76.26	0.04949	8.33	8.42
76.91	0.04721	9.20	8.99
76.91	0.04968	8.22	8.34
76.15	0.04647	9.27	9.25
76.15	0.04777	8.85	8.56
76.15	0.04554	9.75	9.28
76.15	0.04736	8.89	9.06
76.22	0.04800	8.78*	8.78
76.15	0.04632	9.51	9.07
76.22	0.04717	9.10	9.18
76.18	0.04746	8.95	8.97
152.35	0.04752	8.96	9.06
152.35	0.04768	8.94	9.07
152.35	0.04798	9.03	9.00
152.35	0.04680	9.36	9.00
152.35	0.04880	8.47	8.92
152.35	0.04780	8.95	9.14
152.35	0.04788	8.93	9.16
152.42	0.04882	8.94*	8.94
152.35	0.04808	8.78	8.88
152.37	0.04772	8.97	8.88
152.35	0.04824	8.69	8.67
152.42	0.04713	9.27	9.32
152.34	0.04803	8.93	9.31
152.35	0.04752	8.96	9.06
152.39	0.04677	9.16	8.97

* No metering sections densities were available for these points, so the metering section density was taken as the total specimen density.

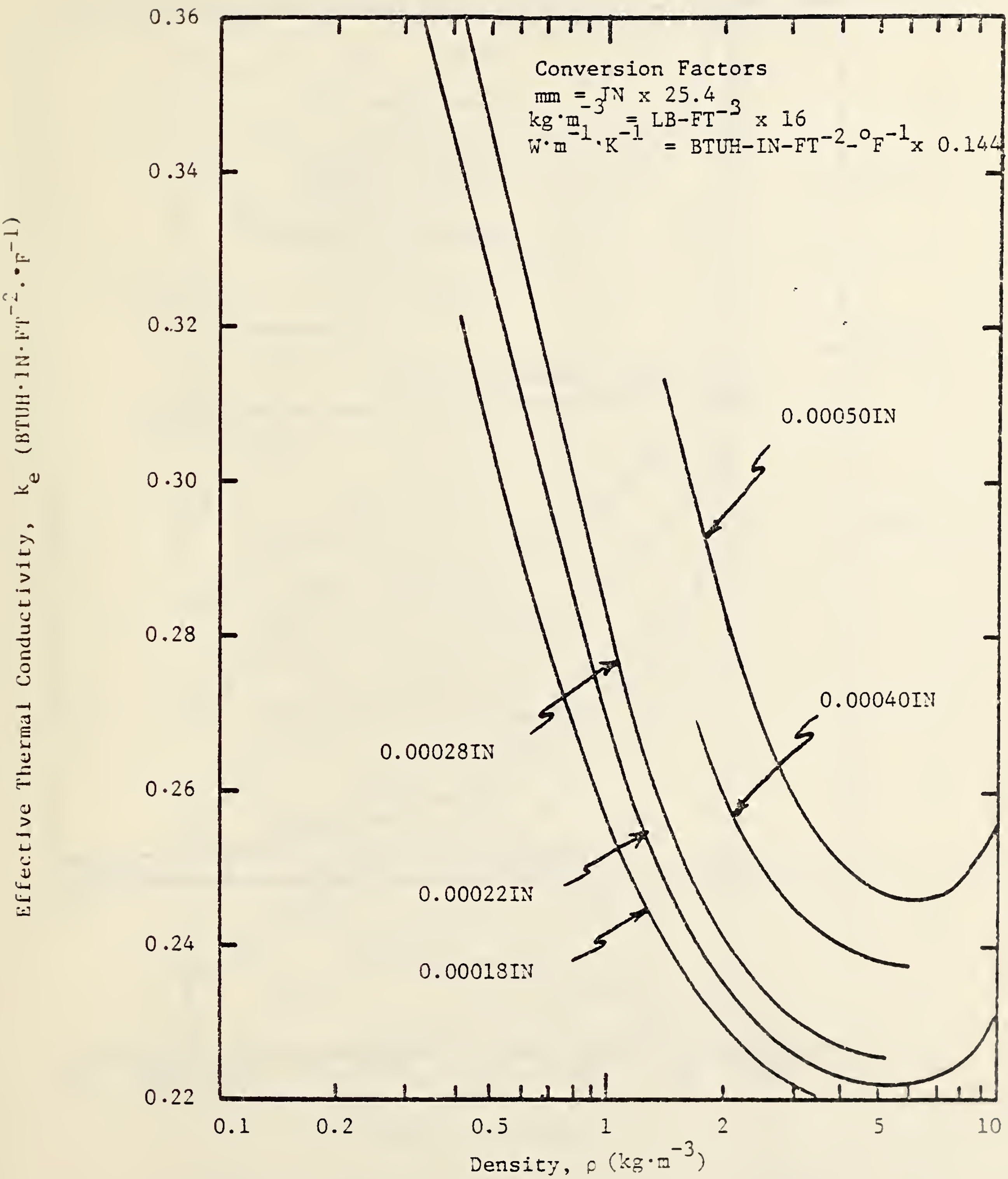

FIGURE 1 THE VARIATION OF THE EFFECTIVE THERMAL CONDUCTIVITY, k_e, WITH THE DENSITY, ρ, AND THE FIBER DIAMETER, δ (ABSTRACTED FROM THE ASHRAE HANDBOOK OF FUNDAMENTALS)

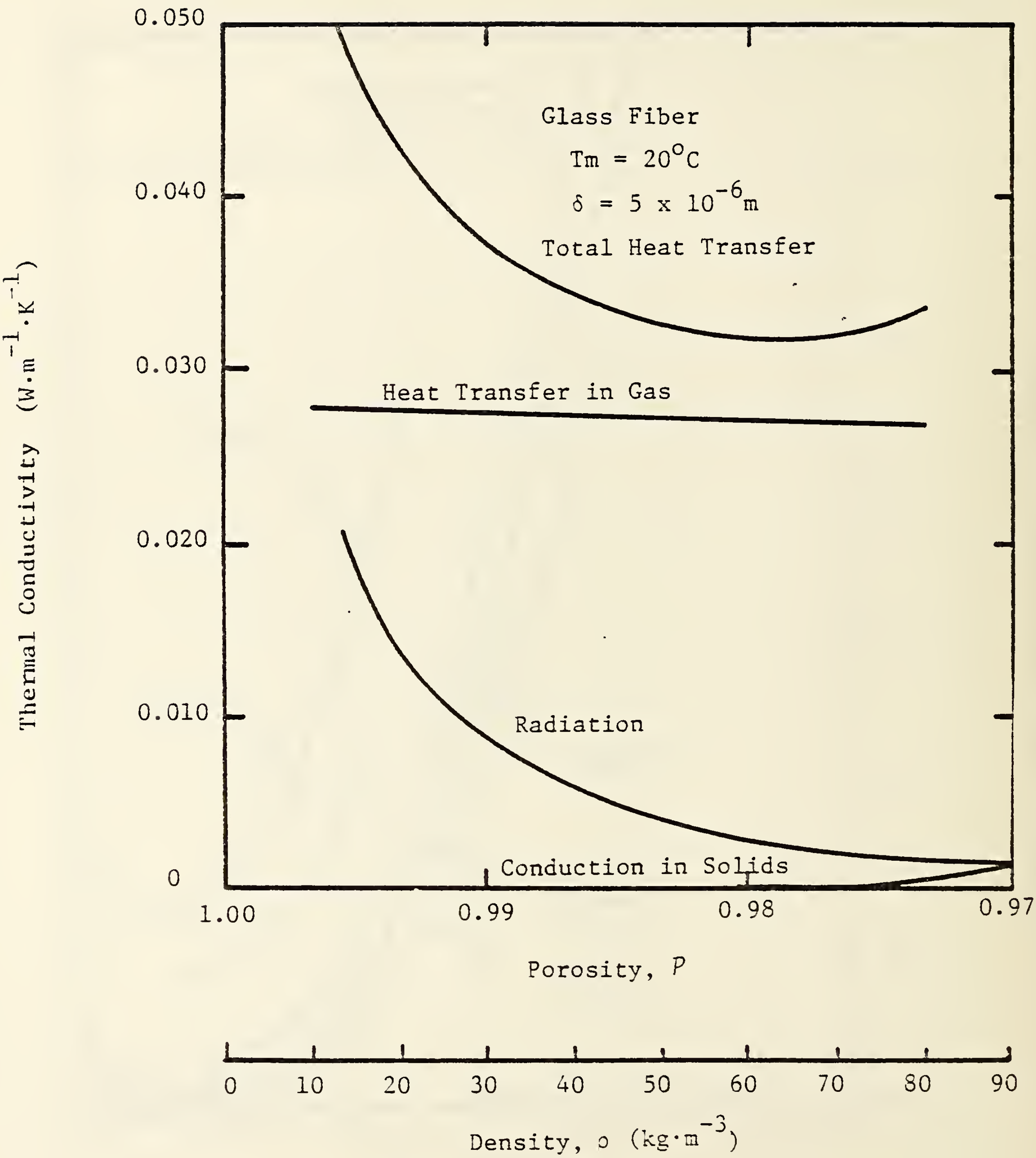

FIGURE 2 THERMAL CONDUCTIVITY VERSUS POROSITY, P, AND DENSITY, ρ (Abstracted from Bankvall [7])

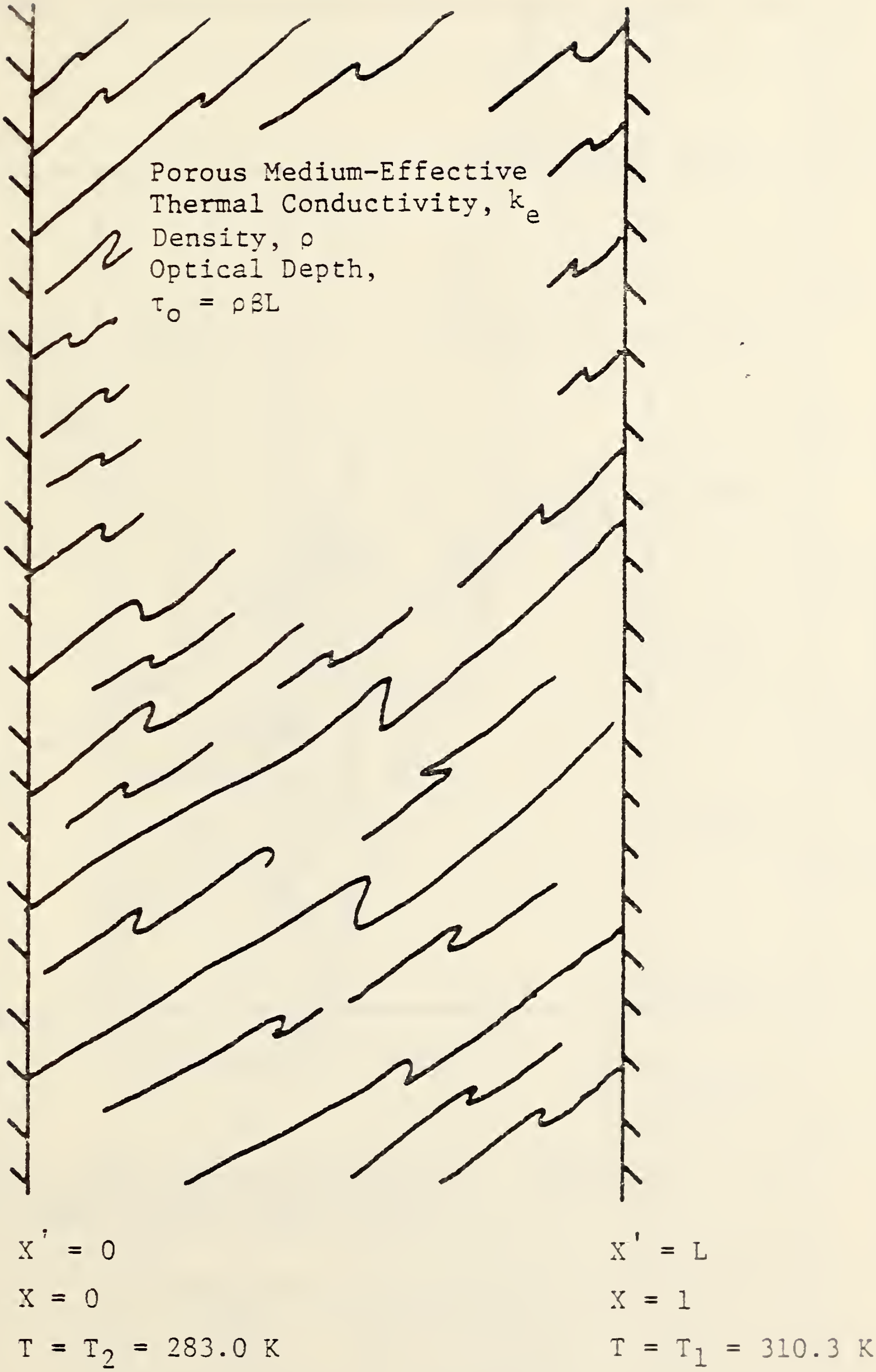

FIGURE 3 THE PHYSICAL SYSTEM

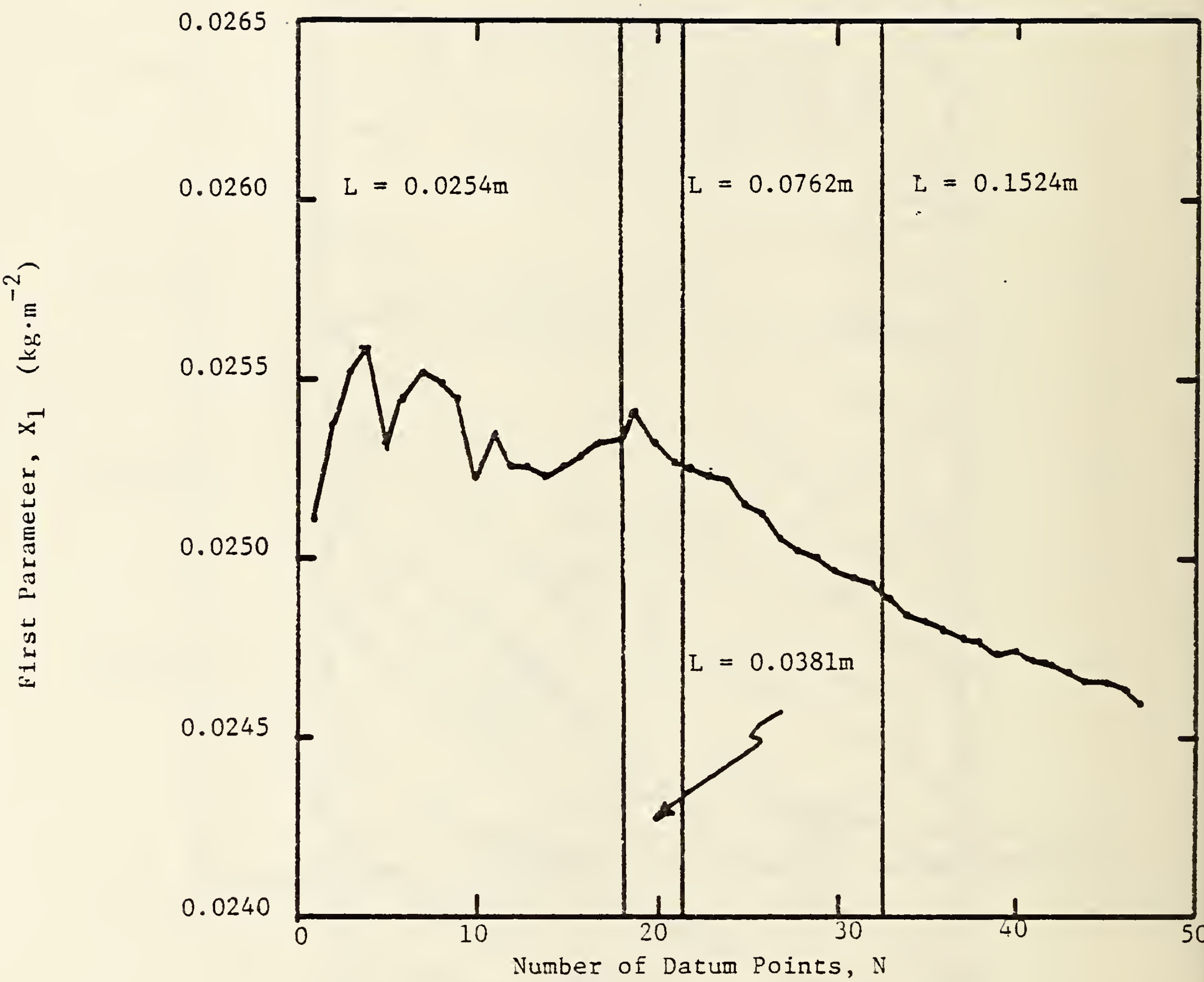

FIGURE 4 THE VARIATION OF THE FIRST PARAMETER, X_1, WITH THE NUMBER OF DATUM POINTS, N

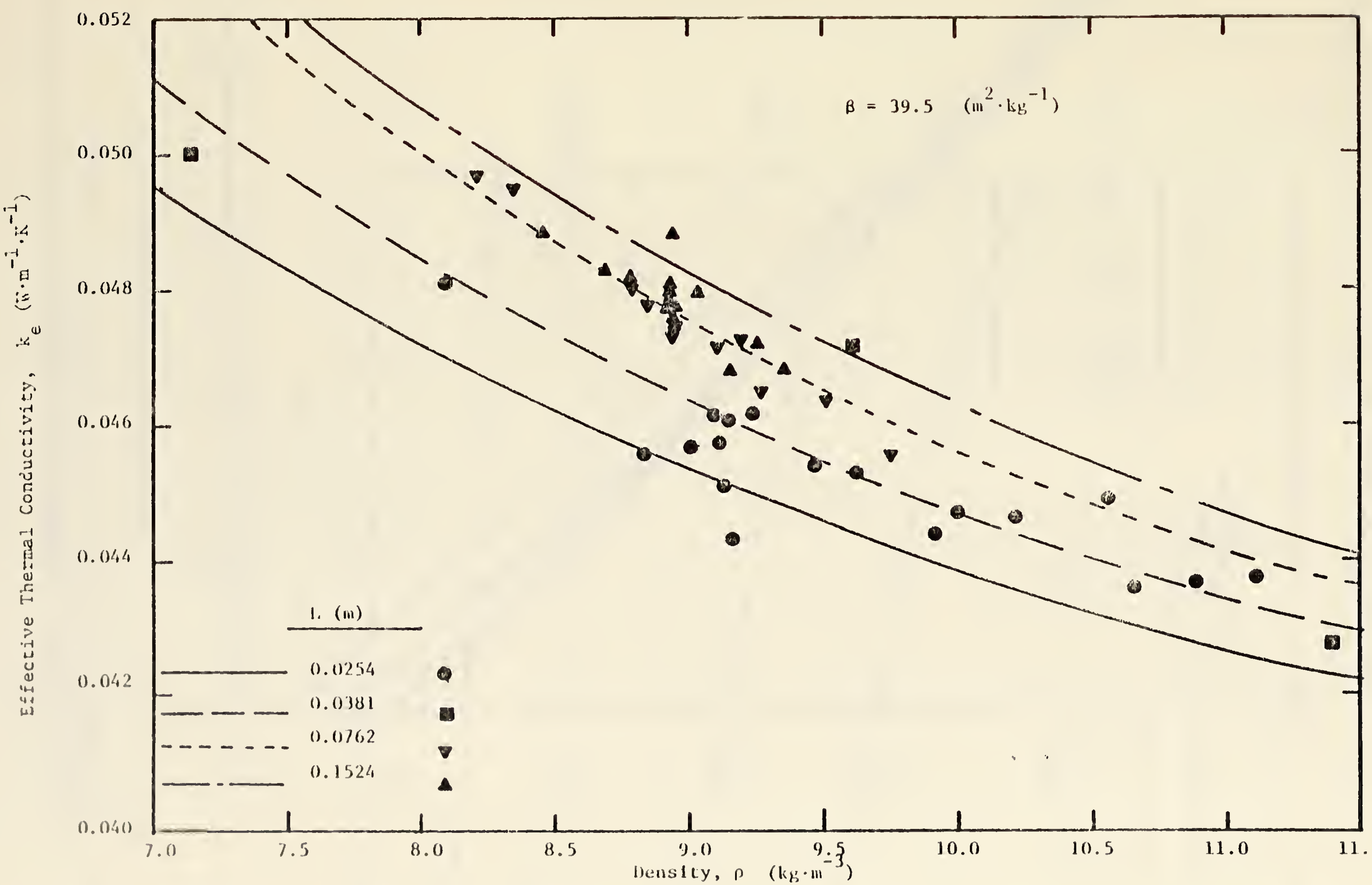

FIGURE 5 THE VARIATION OF THE EFFECTIVE THERMAL CONDUCTIVITY, k_e, WITH DENSITY, ρ, AND THICKNESS, L, FOR THE ONE PARAMETER MODEL

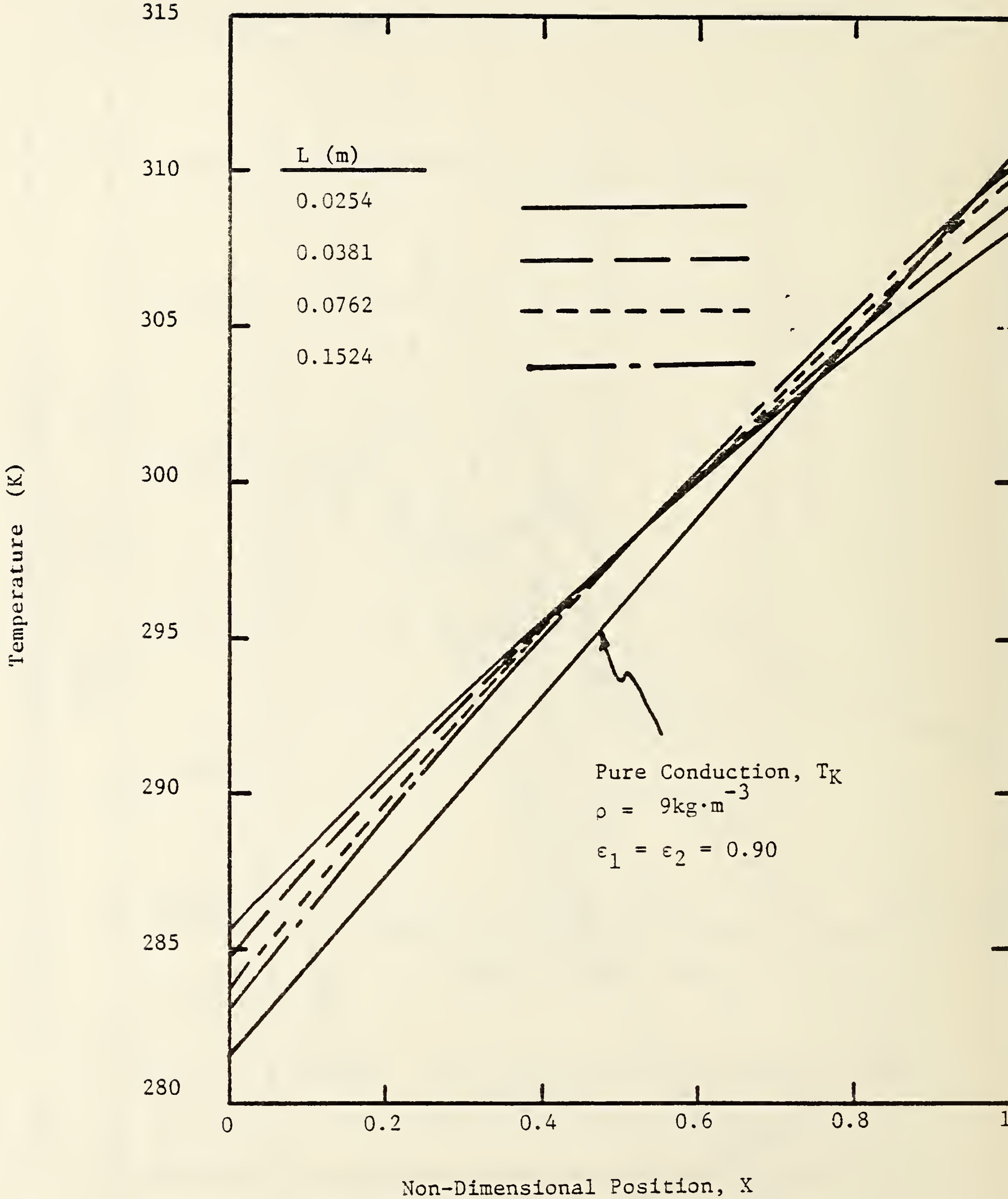

FIGURE 6 TEMPERATURE PROFILES FOR VARIOUS THICKNESSES

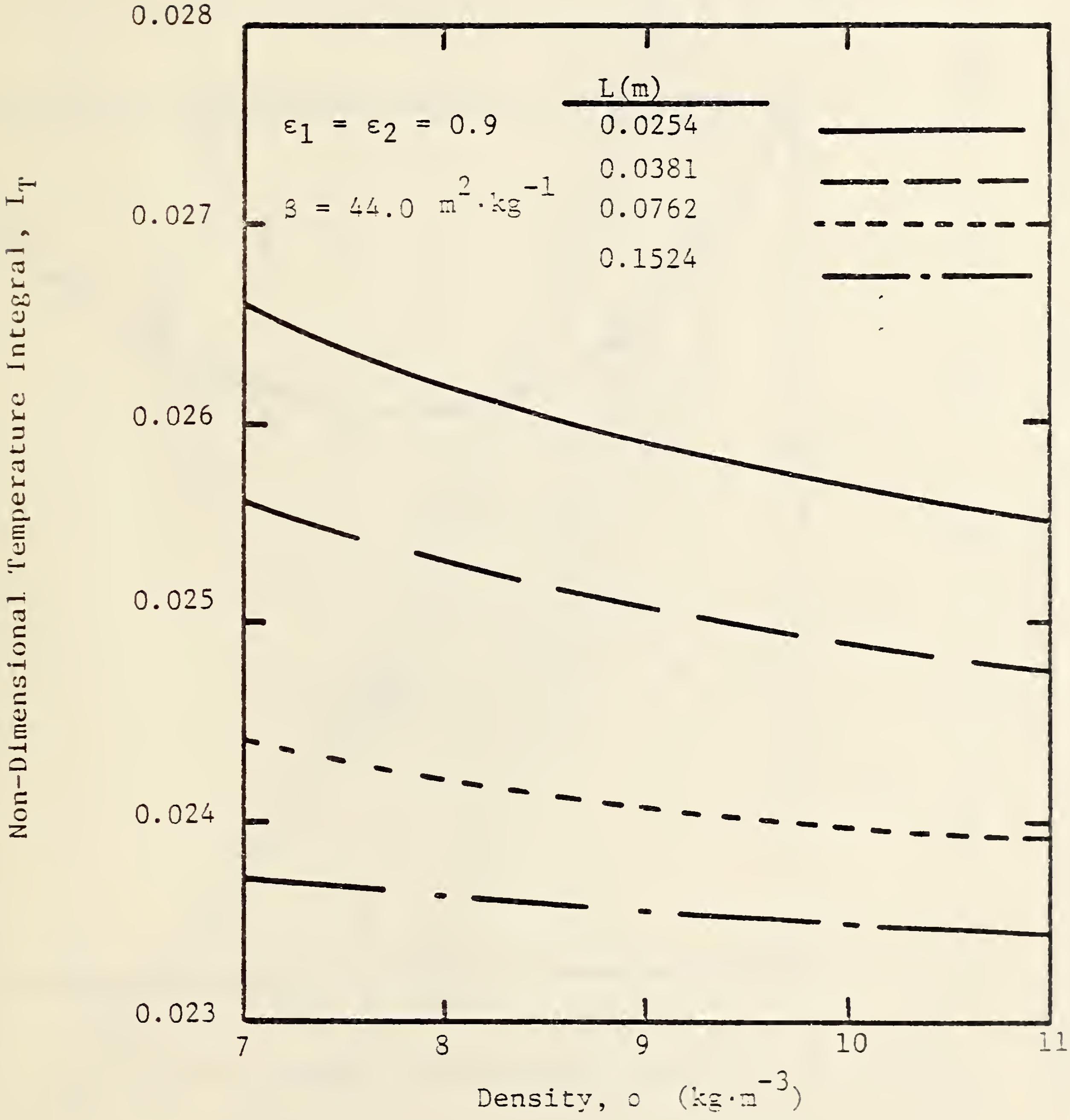

FIGURE 7 THE VARIATION OF THE NON-DIMENSIONAL TEMPERATURE INTEGRAL WITH DENSITY AND THICKNESS

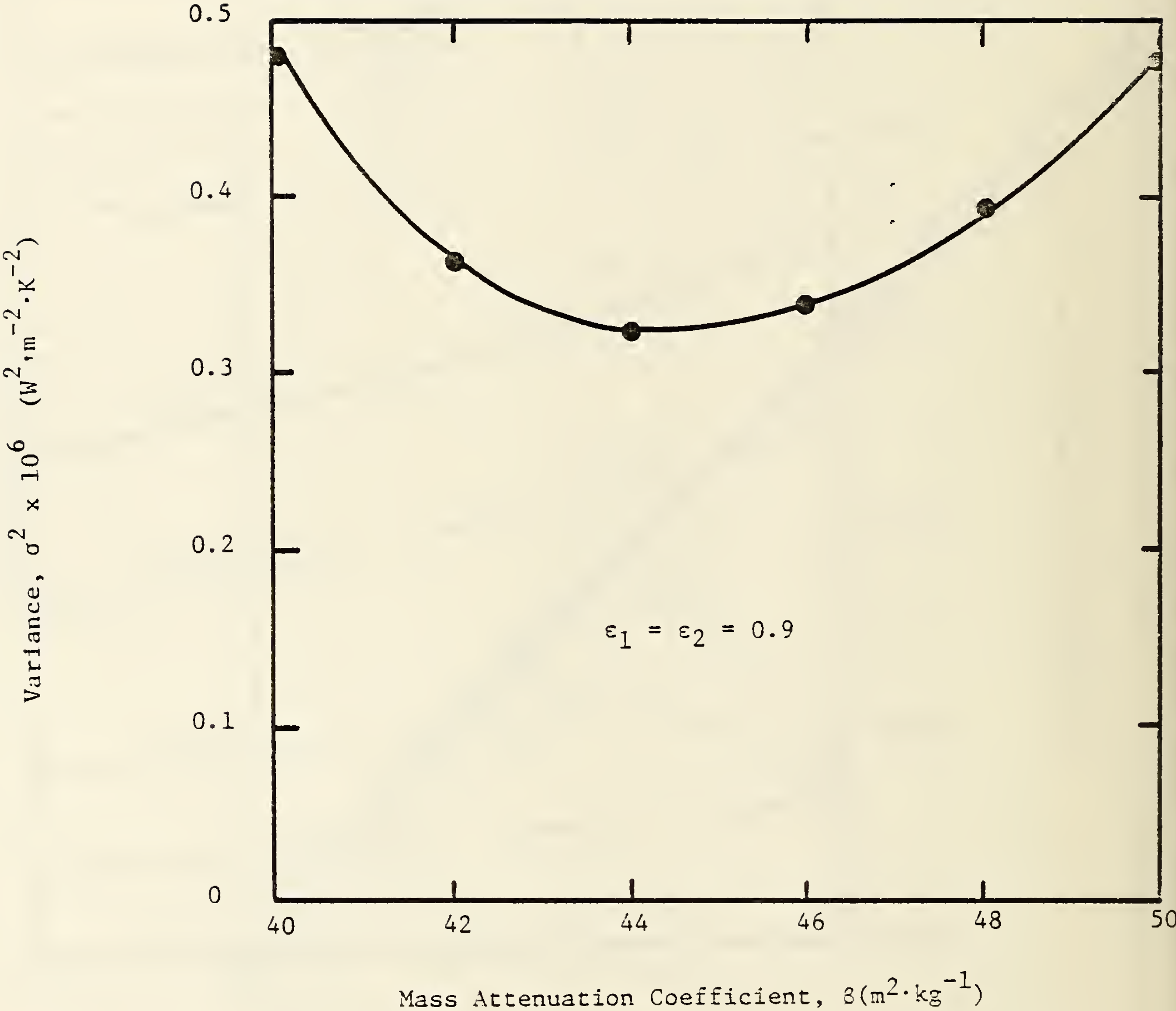

FIGURE 8 THE VARIATION OF THE VARIANCE, σ^2, WITH THE MASS ATTENUATION COEFFICIENT, β

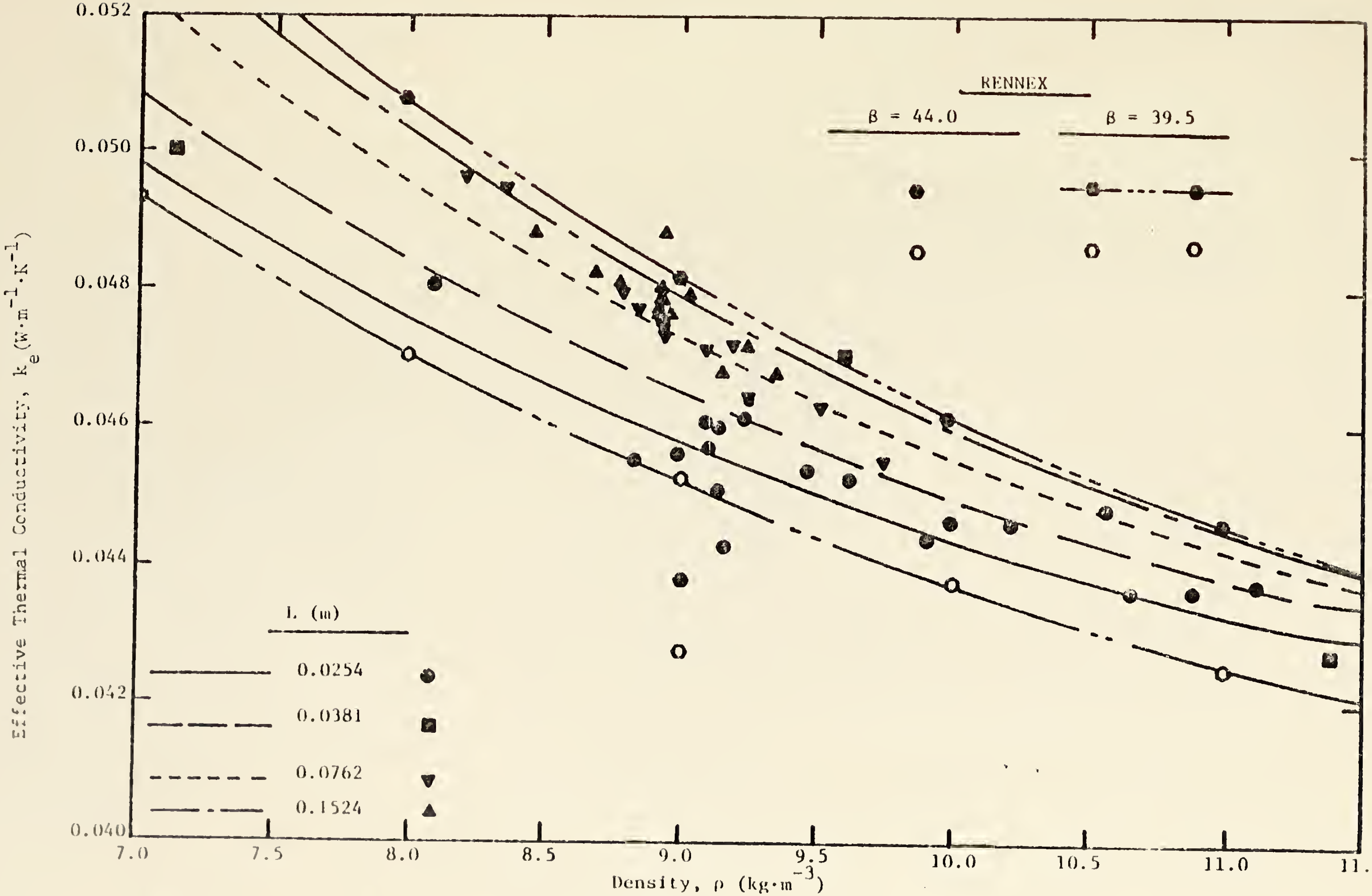

FIGURE 9 THE VARIATION OF THE EFFECTIVE THERMAL CONDUCTIVITY, k_e WITH DENSITY, ρ, AND THICKNESS, L, FOR THE TWO-PARAMETER MODEL

APPENDIX A

LEAST SQUARES DEVELOPMENT

APPENDIX A. LEAST SQUARES DEVELOPMENT

A.1 INTRODUCTION

A formal mathematical development of the sequential least squares algorithm [48] used in this work is presented in this appendix. In the following discussion, matrices will be devoted by upper case letters, vectors by lower case letters with a bar above, and scalars by lower case letters with no bar. All subscripts will refer to order in time or in sequence, although in the general setting of linear systems no reference to time is necessary.

A.2 GENERAL DEVELOPMENT

The general over-determined linear system is given by:

$$A\bar{x} = \bar{y}, \tag{A.1}$$

where A is k x n (k>n) and $\bar{x}$ and $\bar{y}$ are of dimension n and k respectively. In general, no solution exists which satisfies equations (A.1), so it is common practice to choose as a "solution" that value of $\bar{x}$, denoted $x_{l.s}$, which minimizes the functional

$$j = (A\bar{x}-\bar{y})^T (A\bar{x}-\bar{y}) \tag{A.2}$$

I.e. j is the sum of the squared residuals.

The derivation of the least squares solution to equation (A.1) is straightforward, using the following identities for an arbitrary matrix B and vector $\bar{z}$:

$$\frac{\partial(\bar{z}^T B\bar{z})}{\partial z} = 2Bz, \tag{A.3}$$

$$\frac{\partial(\bar{z}^T B)}{\partial z} = B, \tag{A.4}$$

$$\frac{\partial(Bz)}{\partial z} = B^T.$$

To minimize equation (A.2), j is differentiated with respect to x and the derivative $\frac{\partial \gamma}{\partial \bar{x}}$ is set equal to zero.

$$\frac{\partial \gamma}{\partial \bar{x}} = \frac{\partial(\bar{x}^T A^T A \bar{x})}{\partial \bar{x}} - \frac{\partial(\bar{x}^T A^T \bar{y})}{\partial \bar{x}} - \frac{\partial(\bar{y}^T A \bar{x})}{\partial \bar{x}} - \frac{\partial(\bar{y}^T \bar{y})}{\partial \bar{x}}$$

$$= 2A^T A\bar{x} - A^T\bar{y} - (\bar{y}^T A)^T$$

$$= 2A^T A\bar{x} - 2A^T\bar{y}$$

$$= 0 \qquad (A.6)$$

Therefore:

$$\bar{x}_{l.s} = (A^T A)^{-1} A^T\bar{y} \qquad (A.7)$$

A.3 SEQUENTIAL LEAST SQUARES

It is convenient to perform the operations specified by equations (A.7) in a sequential manner, without requiring excessive amounts of computer storage and without necessitating the performance of a matrix inverse as each new row of the system given by equation (A.1) is obtained. To this end, the Woodbury matrix inversion lemma is introduced:

$$(F + BCD)^{-1} = F^{-1} - F^{-1}B(C^{-1} + DF^{-1}B)^{-1}DF^{-1} \qquad (A.8)$$

It is now useful to rewrite equations (A.1) as a block system as follows:

$$\begin{vmatrix} \bar{a}_1 \\ \hline \bar{a}_2 \\ \hline \vdots \\ \hline \bar{a}_k \end{vmatrix} \begin{vmatrix} x_1 \\ x_2 \\ \vdots \\ x_n \end{vmatrix} = \begin{vmatrix} y_1 \\ y_2 \\ \vdots \\ y_k \end{vmatrix} \quad ; \text{ or } A_k\,\bar{x} = \bar{y}_k, \qquad (A.9)$$

where $\bar{a}_i$ represents the $i^{\underline{th}}$ row of the A matrix and A_k represents the A matrix before the $(k+1)^{\underline{th}}$ row has been adjoined to the system.

Assume that for some value of k, the system, equation (A.9), has been solved for $x_{1.s,k}$. When the information $\bar{a}_{k+1}$ and y_{k+1} become available, $\bar{x}_{1.s,k}$ can then be updated to $\bar{x}_{1.s,k+1}$ using equation (A.8).

First, define P_k and $\bar{z}_k$ by:

$$P_k = (A_k^T A_k)^{-1} \text{ and } \bar{z}_k = A_k^T \bar{y}_k \tag{A.10}$$

Then it is seen that for any value of k

$$\bar{x}_{1.s,k} = P_k \bar{z}_k. \tag{A.11}$$

To update P_k and $\bar{z}_k$ to P_{k+1} and $\bar{z}_{k+1}$, note that

$$P_{k+1}{}^{-1} = \left| A_k^T \;\middle|\; \bar{a}_{k+1}^T \right| \left| \begin{array}{c} A_k \\ \hline \bar{a}_{k+1} \end{array} \right|$$

$$= A_k^T A_k + \bar{a}_{k+1}^T \bar{a}_{k+1}$$

$$= P_k{}^{-1} + \bar{a}_{k+1}^T \bar{a}_{k+1} \tag{A.12}$$

with C = 1 in equation (A.8), $P_{k+1} = (P_{k+1}{}^{-1})^{-1}$ can be found as follows:

$$P_{k+1} = P_k - P_k\, \bar{a}_{k+1}^T (1 + \bar{a}_{k+1}\, P_k\, \bar{a}_{k+1}^T)^{-1}\, \bar{a}_{k+1}\, P_k. \tag{A.13}$$

Note in particular that the quality $(1 + \bar{a}_{k+1}\, P_k\, \bar{a}_{k+1}^T)$ is a scaler, so that updating P_k to P_{k+1} requires no matrix inversion.

The vector $\bar{z}$ is also easily updated as follows:

$$z_{k+1} = A_{k+1}^T\, \bar{y}_{k+1}$$

$$= \left| A_k^T \;\middle|\; \bar{a}_{k+1}^T \right| \left| \begin{array}{c} \bar{y}_k \\ \hline y_{k+1} \end{array} \right|$$

$$= A_k^T y_k + \bar{a}_{k+1}^T y_{k+1}$$

$$= z_k + \bar{a}_{k+1}^T y_{k+1} \qquad (A.14)$$

Storage requirements for the above sequential least squares scheme are minimal. The entire A matrix and $\bar{y}$ vector need not be saved; only the relatively small P matrix (n x n) and the $\bar{z}$ vector (dimensional n) need to be saved. As new data arrives it is absorbed by the current P and $\bar{z}$, and the least squares estimate of $\bar{x}$ is kept current.

NBS-114A (REV. 2-80)

U.S. DEPT. OF COMM. BIBLIOGRAPHIC DATA SHEET (See instructions)	1. PUBLICATION OR REPORT NO. NBSIR 84-2906	2. Performing Organ. Report No.	3. Publication Date August 1984

4. TITLE AND SUBTITLE

Thickness Effect in Low-Density Insulation

5. AUTHOR(S)

Patrick J. Burns

6. PERFORMING ORGANIZATION (If joint or other than NBS, see instructions)

NATIONAL BUREAU OF STANDARDS
DEPARTMENT OF COMMERCE
WASHINGTON, D.C. 20234

7. Contract/Grant No.

8. Type of Report & Period Covered

9. SPONSORING ORGANIZATION NAME AND COMPLETE ADDRESS (Street, City, State, ZIP)

National Bureau of Standards
Department of Energy

10. SUPPLEMENTARY NOTES

☐ Document describes a computer program; SF-185, FIPS Software Summary, is attached.

11. ABSTRACT (A 200-word or less factual summary of most significant information. If document includes a significant bibliography or literature survey, mention it here)

A discussion is presented of theory of heat transfer in low-density, glass-fiber insulation via conduction, convection, and radiation. It is concluded that the primary modes of heat transfer in this material are air conduction and radiation. An analysis of NBS data of measured apparent thermal conductivity for different thicknesses results in a parameter estimate of the optical extinction coefficient. This parameter determines the amount of change in apparent thermal conductivity as a function of sample thickness. This phenomena is referred to as the "thickness effect."

12. KEY WORDS (Six to twelve entries; alphabetical order; capitalize only proper names; and separate key words by semicolons)

Conduction; convection; guarded-hot-plate; low-density insulation; thermal conductivity; thermal radiation; thickness effect.

13. AVAILABILITY

[XX] Unlimited

☐ For Official Distribution. Do Not Release to NTIS

☐ Order From Superintendent of Documents, U.S. Government Printing Office, Washington, D.C. 20402.

[X] Order From National Technical Information Service (NTIS), Springfield, VA. 22161

14. NO. OF PRINTED PAGES
46

15. Price
$8.50